

SCIENTIFIC REPORTS



OPEN

Biodegradable Cable-Tie Rapamycin-eluting Stents

Cheng-Hung Lee¹, Ming-Jer Hsieh¹, Shang-Hung Chang¹, Chang-Lin Chiang², Ching-Lung Fan², Shih-Jung Liu^{2,3}, Wei-Jan Chen¹, Chao-Jan Wang⁴, Ming-Yi Hsu⁴, Kuo-Chun Hung¹, Chung-Chuan Chou¹ & Po-Cheng Chang¹

Received: 29 July 2016

Accepted: 8 February 2017

Published online: 08 March 2017

“Cable-tie” type biodegradable stents with drug-eluting nanofiber were developed to treat rabbit denuded arteries in this study. Biodegradable stents were fabricated using poly-L-lactide film following being cut and rolled into a cable-tie type stent. Additionally, drug-eluting biodegradable nanofiber tubes were electrospun from a solution containing poly (lactic-co-glycolic acid), rapamycin, and hexafluoroisopropanol, and then mounted onto the stents. The fabricated rapamycin-eluting cable-tie stents exhibited excellent mechanical properties on evaluation of compression test and collapse pressure, and less than 8% weight loss following being immersed in phosphate-buffered saline for 16 weeks. Furthermore, the biodegradable stents delivered high rapamycin concentrations for over 4 weeks and achieved substantial reductions in intimal hyperplasia associated with elevated heme oxygenase-1 and calponin level on the denuded rabbit arteries during 6 months of follow-up. The drug-eluting cable-tie type stents developed in this study might have high potential impacts for the local drug delivery to treat various vascular diseases.

Percutaneous angioplasty with metallic stents has been used for decades to open up blocked arteries and restore blood flow to the distal circulation that is thought to be causing myocardial or limb ischemia^{1,2}. However, bare metal stents (BMS) have been largely replaced for coronary artery disease (CAD) because drug-eluting stents (DES) have substantially decreased the incidence for repeat revascularization³. Nevertheless, concerns have been raised about delayed endothelialization in DES resulted in the risk of late stent thrombosis^{4,5}. Until healing of the vessel occurs through re-endothelialization, the use of stenting should be non-permanent and limited to following shortly thereafter by the intervention, and responses to the durable polymer could be a problem for chronic inflammation and late stent thrombosis^{6–8}. Hence, subsequent generations of DES have concentrated on biodegradable drug-eluting polymers and the development of biodegradable scaffold-based stents.

Since the first biodegradable stent⁹ in the 1990s, attempts have been made to develop such stents for cardiovascular applications^{10–12}. However, the expansion of most of these stents relies heavily upon the elastic recovery behavior of the polymeric scaffolds. Even though the currently available biodegradable stents have shown relevant products, but still need an advanced manufacturing process¹³ or complex structure which may have stent fracture risk from degradation. Long-term restenosis might happen because of progressive recoil of the polymer-based stents with unsatisfactory elasticity or loss of elastic memory. Recently, a polylactide biodegradable platform eluting drug to treat CAD has desired outcomes comparable with metallic DES^{14–16}. However, clinical trials show that those with a biodegradable vascular scaffold have a greater incidence of incomplete strut apposition and tissue prolapse area. Edge dissection and stent strut fracture may occur, leading to acute stent thrombosis and even death. Furthermore, a direct correlation with stent thrombosis has been observed with increasing extensive procedures, costing on average USD 11,134 per patient^{17–19}.

Hybrid biocompatible nanofiber drug-eluting polymers on BMS and biodegradable-polymer stents have been developed for the application of drugs to repair denuded arteries^{20–22}. In this study, a cable-tie poly-L-lactide (PLLA) stent loaded with rapamycin-eluting poly (lactic-co-glycolic acid) (PLGA) nanofibers was developed to treat denuded rabbit arteries.

¹Division of Cardiology, Department of Internal Medicine, Chang Gung Memorial Hospital-Linkou, Chang Gung University College of Medicine, Taipei, Taiwan. ²Department of Mechanical Engineering, Chang Gung University, Taoyuan, Taiwan. ³Department of Orthopedic Surgery, Chang Gung Memorial Hospital-Linkou, Taoyuan, Taiwan. ⁴Department of Medical Imaging and Intervention, Chang Gung Memorial Hospital-Linkou, Taoyuan, Taiwan. Correspondence and requests for materials should be addressed to S.-J.L. (email: shihjung@mail.cgu.edu.tw)

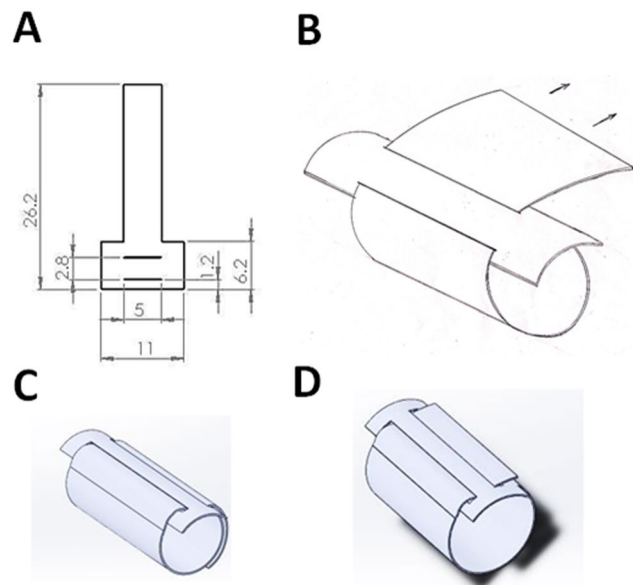


Figure 1. Dimensions of the stent components and the schematic design for self-lock characteristics. The stent element was cut from the film as shown (A). One side of the element (the strip) was glued through the two slits and rolled into a cable-tie type stent as shown (B). Before inflation, the stent can be tied on the preferred balloon size (C). Due to the geometry constraints of the double slits, once the stent is expanded, the strip is not able to slide backward (D).

Materials and Methods

Materials. The biodegradable polymers used in this study were PLLA (Resomer L209S), and PLGA with a poly (lactic acid): poly (glycolic acid) ratio of 75:25 (Resomer RG756S, Boehringer, Germany). We used the anti-proliferative drug rapamycin, and the solvents included chloroform and hexafluoroisopropanol (HFIP) (Sigma-Aldrich, MO, USA).

Biodegradable drug-eluting stents. PLLA film with thickness $60\ \mu\text{m}$ was first prepared using a solvent-casting method with chloroform as the solvent. The stent element was cut from the film as shown in Fig. 1A. One side of the element (the strip) was passed through two slits and rolled into a cable-tie type stent as shown in Fig. 1B. The stent was expanded after being inflated by the balloon (Fig. 1C). Because of geometric constraints of the double slits, the strip could not slide backwards after stent expansion (Fig. 1D). The proposed stent thus exhibited a self-locking characteristic with negligible recoil when subjected to an external force.

Biodegradable nanofibers were prepared using an electrospinning technique. All electrospinning experiments were carried out at room temperature. PLGA (240 mg) and rapamycin (40 mg) were first dissolved in 1 ml of HFIP to electrospin nanofibrous membrane tubes. After electrospinning, the tubes of electrospun nanofibers were then hand crimped and mounted onto the PLLA stents (Fig. 2). All of the biodegradable drug-eluting stents were placed in a vacuum oven at $40\ ^\circ\text{C}$ for three days to let the solvents evaporate.

Group A ($n = 12$) were biodegradable stents with rapamycin loading; and group B ($n = 12$) were stents with no drug loading; and group C ($n = 6$) were BMS (Gazelle, Bare Metal Coronary Stent, Biosensors Europe SA, Switzerland) with rapamycin loading.

Compression test. Compression tests were conducted on a LLOYD tensiometer (AMETEK, USA). A 2500 N load cell was employed with a cross-head speed of $0.1\ \text{cm}/\text{min}$. In radial compression, the stent being tested as well as compressed to deform with different loads (30% reduction in the maximum deflection) was recorded. Five samples were tested for fabricated stents and commercial metallic stents ($3.0 \times 14\ \text{mm}$) (Gazelle, Bare Metal Coronary Stent, Biosensors Europe SA, Switzerland).

Collapse pressure. A self-made system with a flexible Tygon tube attached to a pressure chamber and water circulating flow loop ($37\ ^\circ\text{C}$; $10\ \text{L}/\text{min}$; $76\ \text{mmHg}$) was performed for the collapse pressure of the stents¹³ ($n = 5$).

Weight retention of stent. Weight variation of the stent immersed in the $37\ ^\circ\text{C}$ phosphate-buffered saline (PBS) was calculated. The test stents were taken away from the solution and weighed at different time points following being dried in an oven for one day ($n = 5$).

Microscopic examination. The surface morphology of the electrospun nanofibers and the stents following various times of elution in the buffer solution was examined using scanning electron microscope (SEM) (Hitachi, Ltd, Tokyo, Japan). Diameters and pore space of 100 randomly selected fibers were measured and the average of these measurements gave the diameter and pore space of the nanofibers by ImageJ software (National Institutes of Health, Bethesda, MD, USA).

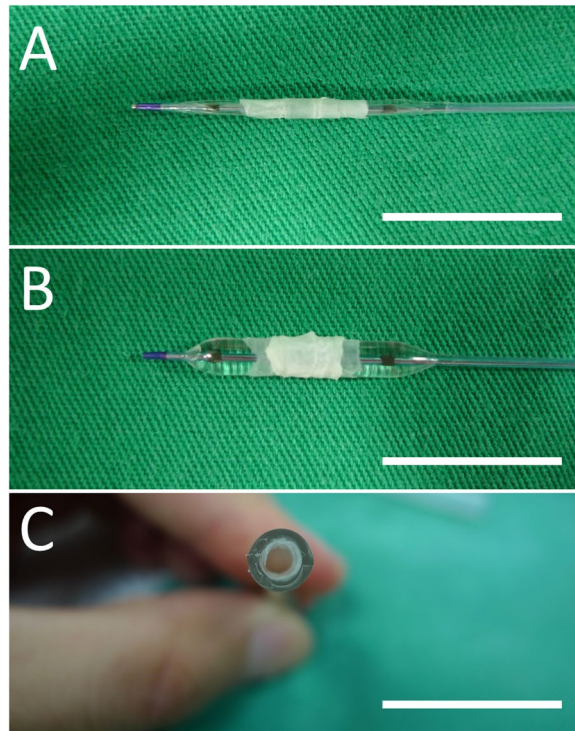


Figure 2. The biodegradable stents (A) before and (B) after expansion by a balloon (C) expansion on plastic tube (Scale bar = 15 mm).

***In-vitro* release of rapamycin.** The glass test tubes with 3 ml of the PBS (0.15 mol/L, pH 7.4) at 37 °C were used for stent incubation and the dissolution sampling. The repeated procedure with adding new PBS (3 ml) for the every 24-hour period was carried out for 4 weeks.

High-performance liquid chromatography (HPLC) study. The release of rapamycin for stents was evaluated using a Hitachi L2400 UV-VIS System (Hitachi, Ltd, Tokyo, Japan). The Hibar C-18, 5 μ m, 4.6 \times 250 mm HPLC column (Merck KGaA, Darmstadt, Germany) was performed for rapamycin separation. The mobile phase had acetonitrile, methanol, and distilled water (40/45/15, v/v/v) at a flow rate of 1.0 ml/min and dissolution sampling (n = 3) was monitored by absorbance at 278 nm.

***In vivo* animal study.** Thirty healthy, adult male New Zealand white rabbits (average weight: 3.4 \pm 0.5 kg) were studied. All experimental procedures were approved by the Institutionally Animal Care and Use Committee of the Chang Gung University, and the aspects of rabbits housing were carried out under the supervision of a licensed veterinarian with the regulations of the Ministry of Health and Welfare, Taiwan.

With oxygen at 2 L/min through a face mask, Xylazine (9.3 mg/kg) (Bayer, Kiel, Gemerny) sedation and tiletamine-zolazepam (10 mg/kg) (VIRBAC, Carros, France) anesthesia were given by intramuscular injection. Group A (n = 12) received biodegradable stents with rapamycin loading; and group B (n = 12) received stents with no drug loading; and group C (n = 6) were treated with BMS with rapamycin loading. Endothelial denudation injury of the artery, and stents implantation procedures were performed as previous studies^{20–22}.

Stented vessels were studied at 6 months after deployment for both inflammatory and injury reactions by histological examinations and microscopic observation^{23,24}. The scale of inflammation was 0 = none; 1 = mild, including minimal infiltrated inflammatory cells; 2 = moderate; 3 = severe with large clusters of inflammatory cells with granulomatous morphology. The scale of vessel injuries were: 0 = strut not in contact with internal elastic lamina (IEL); 1 = strut in contact with IEL and profile in neointima; 2 = strut penetrates IEL with profile in media; 3 = strut penetrates media and is in contact with external elastic lamina, and 4 = strut is in adventitia. The scores of all struts were averaged to obtain the mean score for each of the 24 histological sections.

The ImageJ software was also employed to evaluate the extent of the endothelial surface coverage above the stent struts²⁵. The degrees of cell coverage on randomly selected areas were reported as endothelial coverage percentages. The iE33 ultrasound device (Philips Medical Systems, WA, USA) and angiography were used for hemocompatibility of the implanted stents and patency of the arteries. *In vivo* assessment of endothelial function by trans-abdominal ultrasound was carried out at 4 weeks²⁶. Briefly, endothelium-dependent vasomotor function at the stented segments and at 20–25 mm from the non-stented and non-injured segments as a reference (control) was evaluated following the infusion of two incremental doses of acetylcholine (Sigma-Aldrich, MO, USA) (Ach, 0.05 and 0.5 μ g/mL/min). Additionally, endothelium-independent function was analyzed using nitroglycerine (Nippon Kayaku, Tokyo, Japan) (5 μ g/mL/min)²⁰.

Immunofluorescence and Western Blot Analysis. Optimal Cutting Temperature compound (OCT) (Tissue Tek, Tokyo, Japan) is used to embed tissue samples prior to frozen sectioning on a microtome-cryostat. Frozen sections were washed in PBS for 10 minutes and blocked with 2% bovine serum albumin (Sigma-Aldrich, MO, USA) for 40 minutes at room temperature. The sections were then incubated for one hour at room temperature with primary antibodies against heme oxygenase-1 (Ho-1), and calponin (Abcam, MA, USA, dilution 1:100), and secondary Cy3-conjugated antibody (Thermo Fisher Scientific, MA, USA, dilution 1:100). Nuclei were visualized by DAPI-staining.

Immunoblotting using anti-heme oxygenase-1 (HO-1), anticalponin (Dako), and antiGAPDH (Santa Cruz, Delaware Ave, CA) antibodies as primary antibodies was carried out. The amount of the proteins which were relative to GAPDH was analyzed using the enhanced chemiluminescence-detection method (Amersham, Netherlands) and quantified by densitometry.

Statistics and data analysis. Statistical analysis was conducted with SPSS software (version 17.0 for Windows; SPSS Inc., Illinois, USA). All data are presented as means \pm standard deviation. One-way ANOVA, followed by *post hoc* Bonferroni analysis for pairwise comparisons was used to compare the data for statistical significance. Differences were considered statistically significant at a *p* value of less than 0.05.

Results

Using solvent-casting and electrospinning techniques, we successfully fabricated biodegradable drug-eluting stents. These biodegradable stents were passed over a commercial balloon dilatation catheter (Voyager NC Coronary Balloon Catheter 3.0×15 mm, Abbott Vascular, CA, USA) (Fig. 2A), and then placed inside a flexible plastic tube (3.0 mm) for inflation using a manual balloon catheter pump (Perouse Medical, France). The fabricated stents with the nanofibers were expanded with the force exertion by the balloon (8 atm) (Fig. 2B). The recoils of group A and B stents in the longitudinal dimension after expansion were comparable (diameter 3.09 ± 0.11 mm vs. 3.04 ± 0.13 mm, $p = 0.543$). A “cable-tie” type stent with an internal diameter of 3.0 mm and an outer layer of rapamycin-eluting nanofibers was thus achieved. The stent still attached to the plastic tube following balloon pressure release and remove because of the anti-recoil property of the stent design (Fig. 2C).

Figure 3 shows electrospun drug-eluting nanofibers (5,000X) using the SEM micrograph. The mean diameter of the nanofibers in group A (695.4 ± 98.8 nm) was significantly lower than that in group B (780.5 ± 226.9 nm) ($p = 0.001$) (Fig. 3B and E), however the pore space in group A ($6701.2 \pm 2683.7 \times 10^3$ nm²) was significantly larger than that in group B ($2196.4 \pm 936.3 \times 10^3$ nm²) (Fig. 3C and F) ($p < 0.001$).

Characteristics of the fabricated stents. Tensile tester was used for compression strength of the fabricated stents to compare with that of metallic stents with maximum 30% compression strain (Fig. 4). As expected, the biodegradable stents had an inferior compression strength (0.48 ± 0.25 N) to the metallic stents (1.84 ± 0.47 N) on 30% load ($p < 0.001$) (initial diameter of the cable tie DES and BMS: B and D; maximum 30% compression load: C and E).

Both metallic and fabricated stents were also measured for collapse pressures. The collapse pressure of the metallic stent was 2.53 ± 0.11 kg/cm², compared to 1.36 ± 0.14 kg/cm² of the cable-tie biodegradable stent ($p < 0.001$). Figure 5 shows variations in weight of the fabricated stents with time. The weight of the biodegradable stents decreased to $92 \pm 1.3\%$ at 16 weeks, indicating that they underwent material degradation over time.

The surface of a newly fabricated PLLA stent is presented using SEM in Fig. 6. The surface was smooth, despite some roughness that was due to the mold surface during the solvent casting process (Fig. 6A). Figure 6B shows micrographs of a fabricated stent after 16 weeks elution in PBS at 37 °C. On surface area, no significant appearances of stent degradation on surface were noted (500X) according to SEM.

In vitro release of rapamycin. HPLC analysis suggested that the release curve of the biodegradable stents involved two stages of rapamycin release: an initial burst, and a rather steady degradation-controlled drug release (Fig. 7). Only 40% of the drugs were detected for the first 28 days, indicating that the drug-eluting nanofiber could effectively release rapamycin for more than four weeks.

In vivo efficacy of the biodegradable stents. *In vivo* studies were evaluated using 30 rabbits that treated biodegradable cable-tie stents loaded with or without rapamycin or BMS with rapamycin in the denuded descending abdominal aorta. The vessel position and stent deployment were verified via angiography in each animal during the procedure. Since the stents themselves (arrowheads) could not be visualized under X-rays, we mounted a platinum marker bead (arrow) in the struts of the middle section (Fig. 8).

Figure 9 shows the observed endothelial coverage of the animals' arteries. At 6 months, the surfaces of the struts were completely covered with regularly shaped endothelia in close contact with each other (300X) (Fig. 9A and B) (Endothelial coverage percentage: group A 97.1 ± 1.5 , group B 97.3 ± 1.3 , group C 96.2 ± 0.9 , Anova $p = 0.145$) (Fig. 9A). Therefore, re-endothelialization on the surfaces of the struts and the endothelia of group A were aligned in the direction of the flow and comparable with those of group B with no drug loading (1000X) (Fig. 9B).

Following incision of the aorta, the implanted stents were found to be intact. Additionally, no thrombus formation in the stent-implanted vessels was noted in the photomicrographs of cross-sections (Fig. 10). By week 24, group A exhibited re-constituted and regenerated endothelium without substantial intimal hyperplasia (Fig. 10A), whereas group B demonstrated significant intimal hyperplasia (Fig. 10B, double arrow). No significant variation for inflammatory response was detected among the three groups of rabbits (1.5 ± 0.5 vs. 1.4 ± 0.5 vs. 1.6 ± 0.5) (ANOVA $p = 0.694$). Vascular injury scores were also comparable at 24 weeks (2.4 ± 1.1 vs. 1.7 ± 0.8 vs. 2.4 ± 0.9) (ANOVA $p = 0.165$).

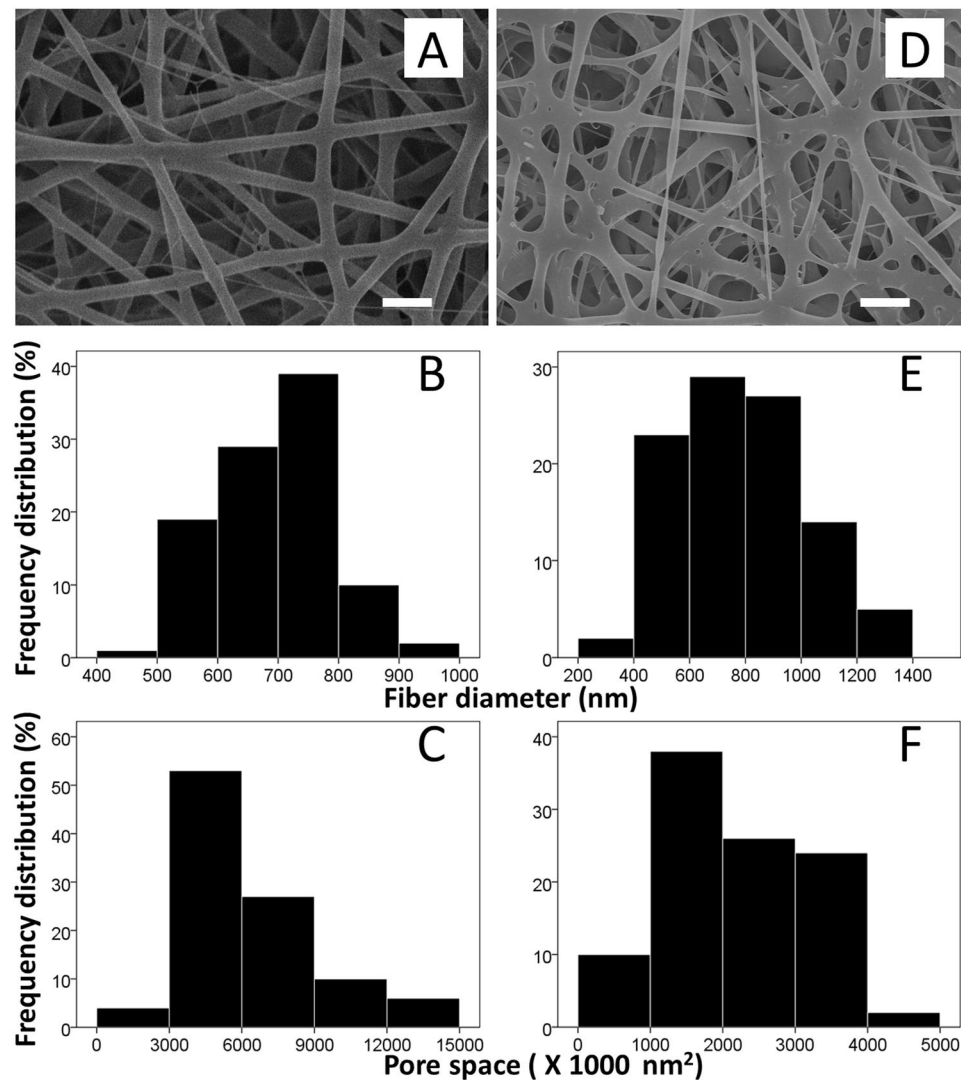


Figure 3. SEM view of electrospun drug-eluting nanofibers ($n = 100$ in each group) (A) rapamycin; and (D), PLGA only) and their frequency distribution of fiber diameter (B and E) as well as pore space (C and F) (Scale bar $2.5 \mu\text{m}$).

Immunofluorescent labeling of HO-1 and calponin were detected on stented arteries using confocal fluorescence microscopy. HO-1 (Fig. 11) and calponin (Fig. 12) labeling index of the interstitial of intima and elastic lamina of the artery were measured as the ratio of density staining for both markers to DAPI-labeled nuclei. At month six, both groups exhibited significantly higher amount of HO-1 and calponin than did those in the group B (HO-1: group A 0.64 ± 0.02 , group B 0.35 ± 0.03 ; Calponin: group A 0.29 ± 0.02 , group B 0.21 ± 0.03) (p all < 0.001). In Fig. 13, immunoblotting of level of HO-1 and calponin also was elevated on group A comparing with group B ($p = 0.005$ and $p = 0.037$, respectively).

Six months after the deployment of the fabricated stents, no migration of the implanted stents was observed. In addition, studies using trans-abdominal vascular ultrasound and angiography showed that the stents were all patent in the test rabbits (Supplemental Video).

Endothelial function was assessed following 28 days of stent deployment, and the response of an endothelia-dependent vasodilatation to Ach was significantly stronger in the rabbits that received cable-tie DES than in those in group C (*post hoc* $p < 0.001$). The cable-tie rapamycin-eluting biodegradable stents also exhibited a comparable vasodilatory response to the control group (non-injured vessels) (*post hoc* $p = 0.241$ and 0.902 with Ach 0.05 and $0.5 \mu\text{g}/\text{min}/\text{kg}$ infusion, respectively) (Fig. 14).

Discussion

Routine implantation of balloon-expandable stents to achieve optimal stent dimensions has been reported to improve late clinical and angiographic outcomes^{27,28}. The biodegradable rapamycin-eluting stent that we developed in this study is designed to be expanded by a balloon, and has a self-locking characteristic which can avoid stent recoil resulted from polymer properties and the external pressure of the arteries. The use of oversized

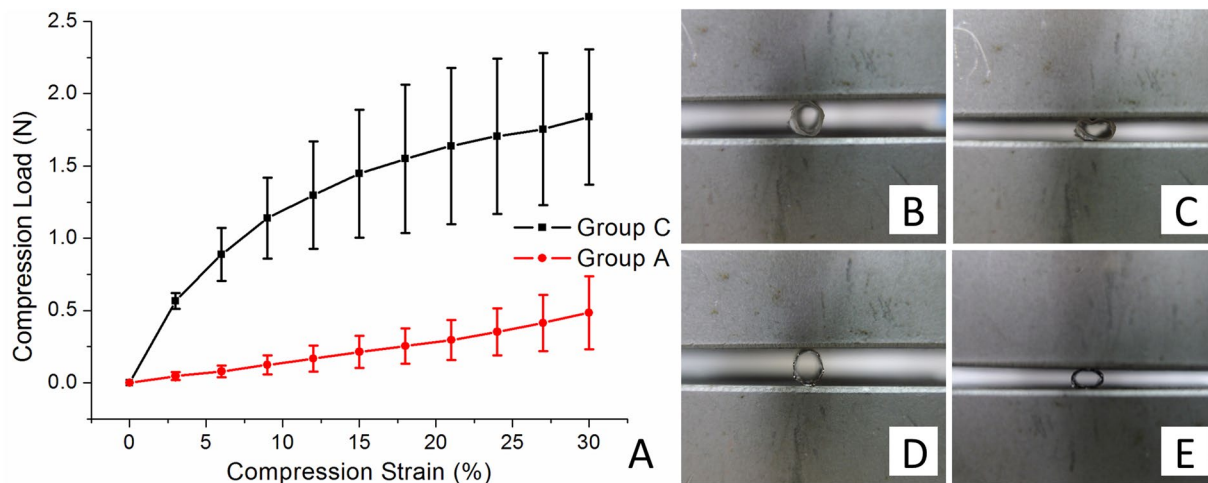


Figure 4. A comparison of the biodegradable stents (n = 5) and the metallic stents (n = 5) under the compression test (A) with maximum 30% compression strain (Initial diameter of the cable tie DES and BMS: (B and D) maximum 30% compression load: (C and E).

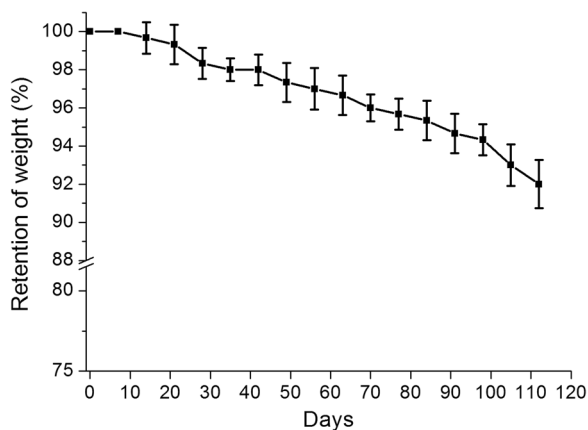


Figure 5. Weight change of the biodegradable stents with time (n = 5).

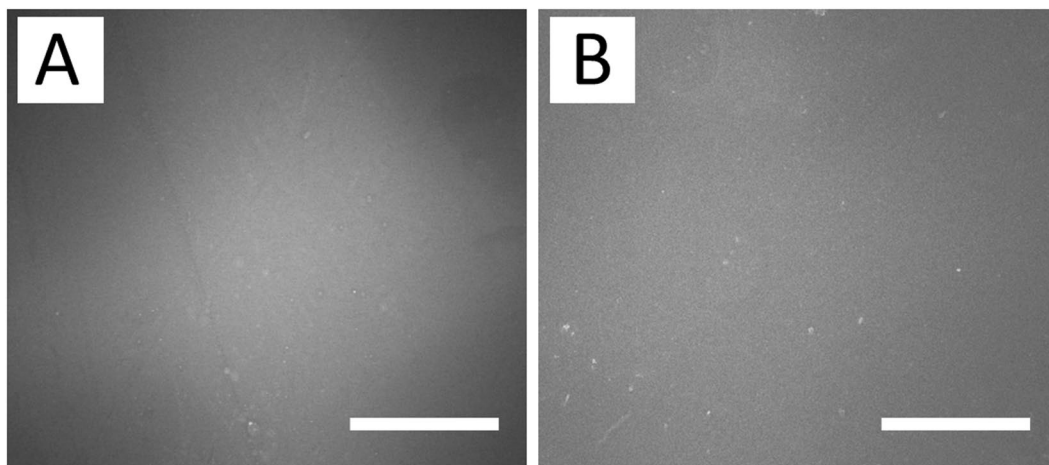


Figure 6. SEM photo of the stent surface, (A) before elution, and (B) 16 weeks after the elution process (n = 5) (scale bar = 50 μm).

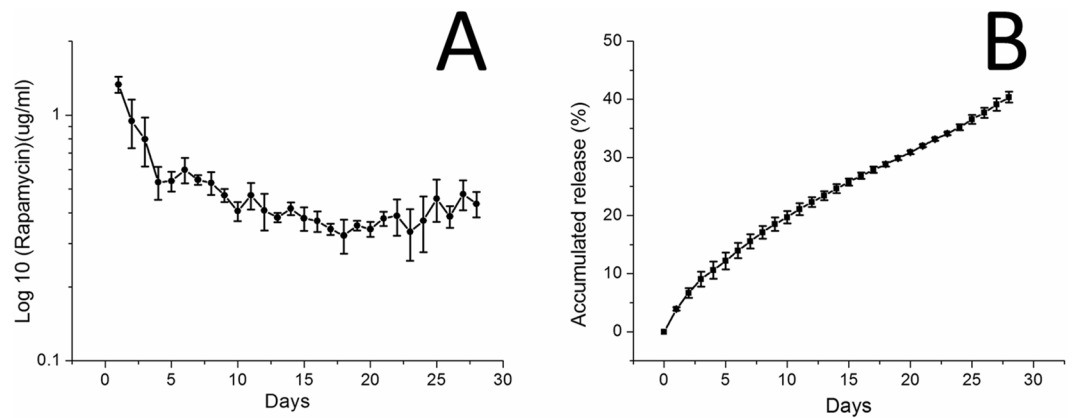


Figure 7. (A) Daily and (B) accumulated release curves of rapamycin from the biodegradable drug-eluting stents.

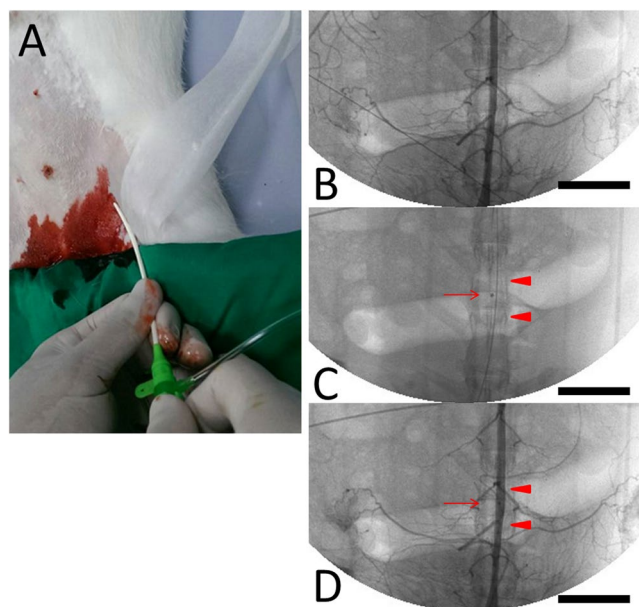


Figure 8. Using the puncture technique, a 6F sheath was inserted into the femoral artery (A). Biodegradable stents (arrowheads) with a single central radiopaque platinum marker (arrow), mounted and loaded with rapamycin nanofibers ($6\mu\text{g}/\text{mm}^2$) were implanted in the abdominal aorta of the rabbit (B,C,D) (Scale bar = 20 mm).

balloons and high pressures of inflation can result in late lumen loss and neointimal proliferation. Several studies have confirmed that the main predictors of freedom from restenosis following stent implantation are the minimal luminal area and diameter achieved^{29,30}. In this study, the stent struts become completely expanded and fully apposed at 8 atm, which is comparable to the pressure performed for the nominal pressure at which expands to its named balloon diameter and needed for present stent deployment^{10,31}. Due to the self-locking design, changes in longitudinal dimensions of the fabricated stents following expansion are insignificant. Therefore, the delivery and deployment systems for our proposed stent are using similar deployment techniques and thereby hastening clinical acceptance for endoluminal deployment.

Sufficient radial forces are a crucial element of biodegradable stents, which are anticipated to display minimum radial recoil and high radial force when implanted in various advanced atherosclerotic lesions³². Neither the collapse pressure nor compressive strength of our fabricated biodegradable stents reduced significantly after immersion in buffer solution, which demonstrated that these characteristics remained almost unaltered in all the study period. The ultimate collapse pressure needed to oppose arterial blood vessel pressure was 3×10^4 Pa ($0.31 \text{ kg}/\text{cm}^2$)³³, which is lower than the pressure of our PLLA biodegradable stent design (around $1.36 \text{ kg}/\text{cm}^2$). The collapse pressure of our polymeric stent was also markedly higher than the human physiological pressure ($1.02 \text{ kg}/\text{cm}^2$)¹². In addition, no significant reduction in weight was noted in the stents after immersion in PBS for

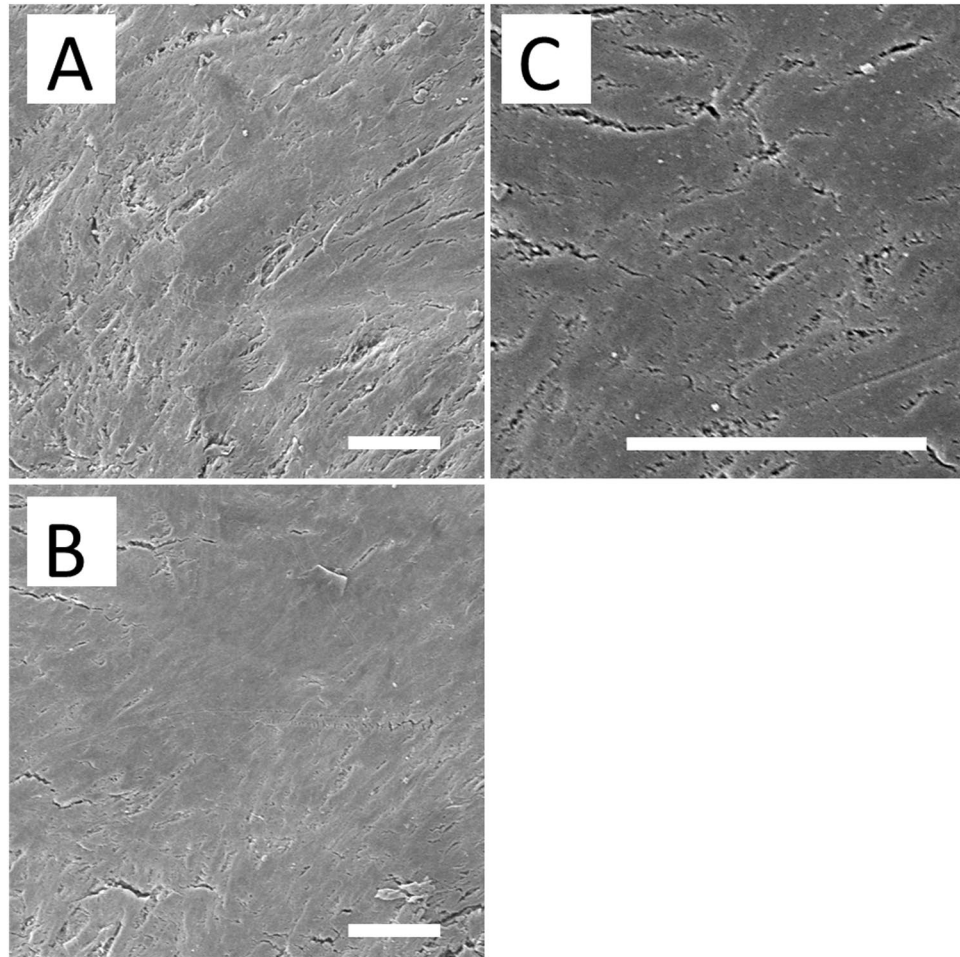


Figure 9. At 6 months, the surfaces of the struts were completely covered with regularly shaped endothelia in close contact with each other in Group A and B (300X) (A and B). Furthermore, re-endothelialization on the surfaces of struts among and the endothelia of group A were aligned in the direction of the flow (1000X) (C). (Scale bar = 50 μm).

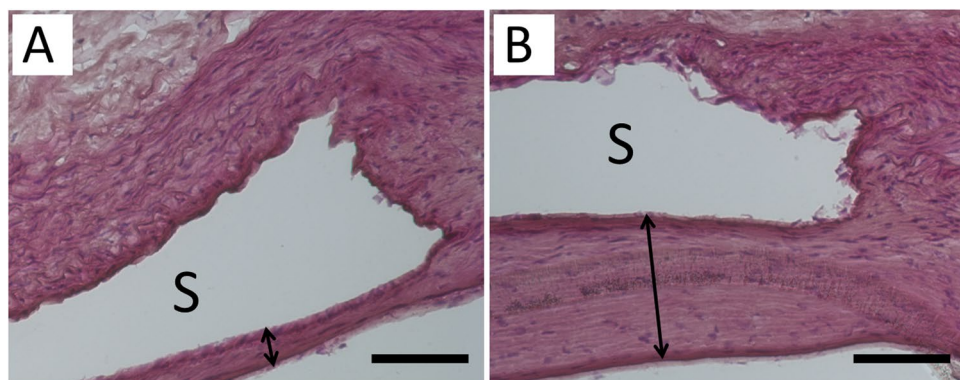


Figure 10. By weeks 24, group A exhibited re-constituted endothelium with insignificant intimal hyperplasia (A) however, group B showed substantial intimal hyperplasia with a thickness of around 70 μm (B) (double arrow). (Scale bar = 50 μm) (S: stent strut).

16 weeks. This may be because the total degradation time of PLLA has been reported to be more than 2 years^{34,35}, which indicates that minimal degradation and water uptake takes place to initiate hydrolysis of PLLA.

Rapamycin is an effective immunosuppressant and retains both antineoplastic and antifungal properties. Rapamycin for local anti-proliferative therapy can inhibit the migration and growth of arterial smooth muscle

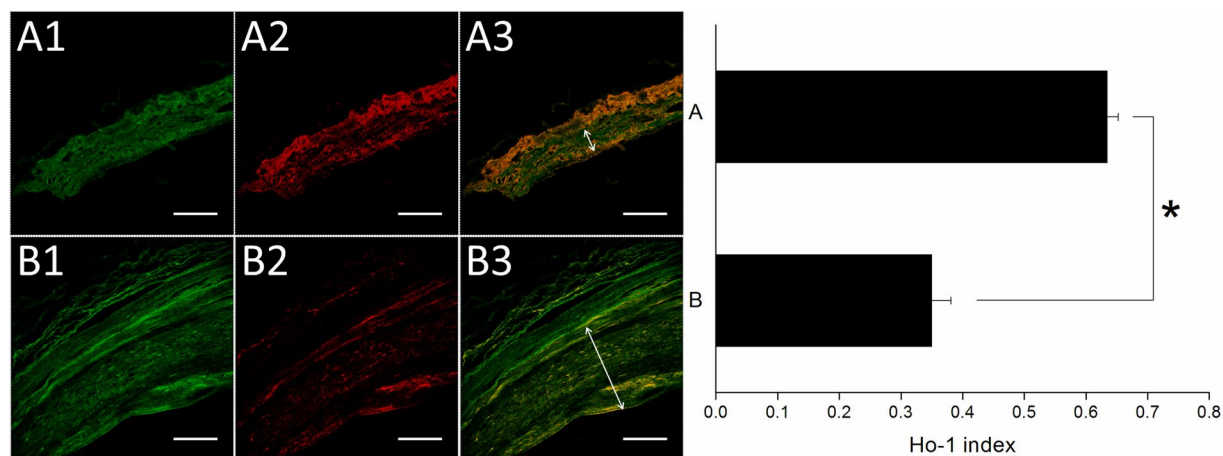


Figure 11. Immunofluorescence of Ho-1 on stented arteries following 24 weeks. Ho-1 immunostaining (red) of group A (A) and group B (B) stented region and autofluorescence on tunica media (green) were also shown. Great expression of positive labeling with Ho-1 was detected on the rapamycin-eluting cable tie stented vessels. The double arrow illustrates tunica media. Group B showed that substantial neointimal hyperplasia (Scale bar = 150 μm).

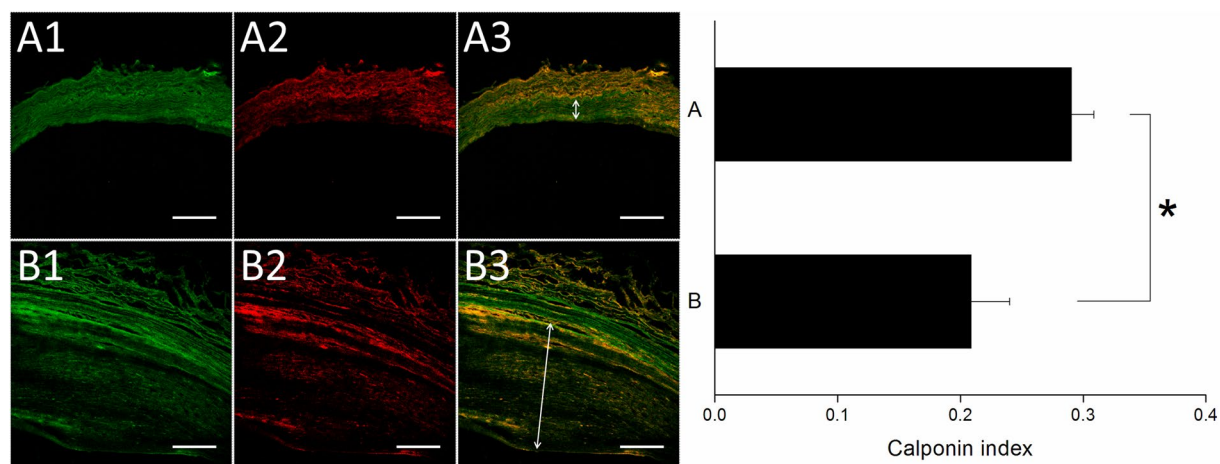


Figure 12. Calponin immunostaining (red) of group A and group B was shown. Less degree of positive labeling with calponin was shown on group B after 24 weeks. The double arrow also depicts tunica media. (Scale bar = 150 μm).

cell, and prevent intimal hyperplasia from restenosis after balloon angioplasty^{36,37}. The sustained release of rapamycin from our biodegradable stents could significantly decrease smooth muscle cell growth as well as reduce inflammatory reactions *in vivo*, which are the main reasons of stent restenosis and neointimal proliferation.

In this study, PLGA was electrospun into nanofibers to elute rapamycin onto the surface of biodegradable cable-tie stents to deliver drug locally. The fiber diameters reduced with the addition of rapamycin. This might be due to the fact that the polymer concentration in the PLGA solution decreases with the addition of the drugs. The solution thus has less strength to resist the action of the external stretching force by the electrical field during electrospinning. Electrospun fiber diameters decreased accordingly. Many various polymeric ingredients are used because of they can perform a continuous delivery of pharmaceuticals, of which PLGA is the most promising biodegradable bio-material because of non-toxic and minimal inflammatory responses. Venkatraman *et al.* developed drug-eluting biodegradable stents using a solvent-casting method, and reported that the collapse pressure of PLLA stents reduced with a more significant decrease at a higher level of drug combination³⁸. Therefore, drug concentrations should be restricted to less than 1 wt% to maintain the mechanical characteristics of the PLLA matrix. The use of electrospun nanofibers has advantage of the increased drug loading of the PLLA stent with no significant decrease in mechanical strength. The experimental results of this study also indicated that the biodegradable stents could release an effective and high concentration of rapamycin for over 4 weeks. Furthermore, by using electrospun nanofibers, the initial burst delivery of rapamycin amount was small, thereby avoiding the possible toxicity related to rapamycin³⁹ and adding benefits in the light of constant drug delivery for vascular uses.

HO-1 is an adaptive enzyme, whose production is triggered in oxidative stress-induced inflammatory⁴⁰. HO-1 has directly effects on the vasoconstriction reduction and cell proliferation inhibition during vascular injury⁴¹.

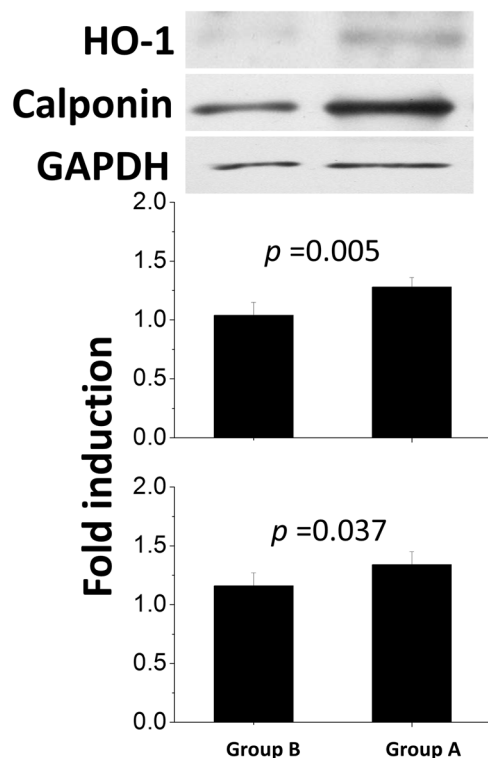


Figure 13. Quantitative analysis of HO-1 and calponin content of arteries in groups A and B at week 24.

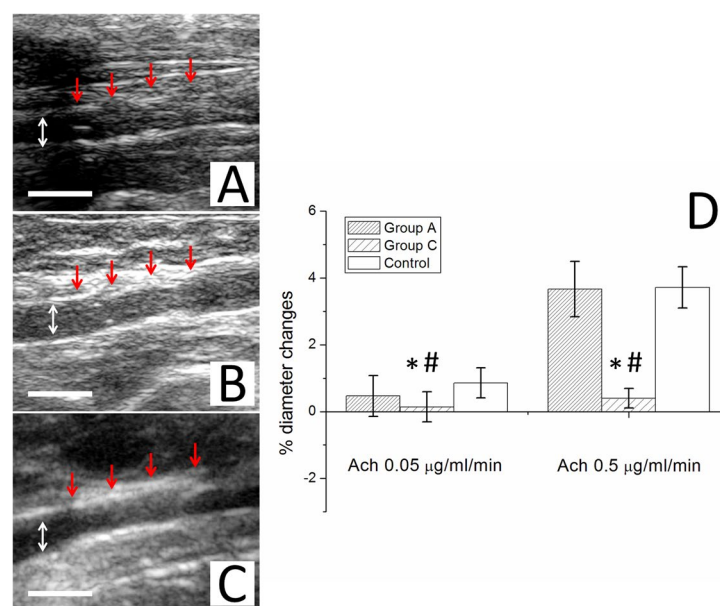


Figure 14. One week (A) and 4 weeks (B) group A; C: group C) following the procedure, no migration and patent abdominal aorta were observed for the implanted stent (arrow) using the vascular ultrasound. (Scale bar = 5 mm) ($*P < 0.05$ group A versus group C) in post hoc analysis; ($\#P < 0.05$ group C versus control group) in post hoc analysis).

Vascular wound healing considered as local reparative inflammatory responses implicates an essential protective role for HO-1 in arterial vascular disease. Additionally, rapamycin has therapeutic effect on the induction of HO-1 expression for the antiproliferative actions⁴². Calponin, a vascular smooth muscle cell differentiation marker, is a protein associated with actin, calmodulin, and tropomyosin and is involved in the ancillary role of

smooth muscle cell contraction^{43,44}. Expression of the calponin is reduced in proliferating smooth muscle cells and resultant atherosclerotic neointima in response to injured arterial media^{45,46}. Hence, rapamycin can promote and induce vascular smooth muscle cell differentiation with increased calponin and is an inhibitor of in-stent restenosis resulted from vascular smooth muscle cell proliferation⁴⁷.

There are some limits to this study. First, only a relatively small number of experimental animals were included, and we used denuded rabbit aortas without pre-existing atherosclerotic lesions. Second, the follow-up period in our study was 6 months after cable-tie stent implantation, and thus it remains unknown whether endothelial dysfunction associated with rapamycin release persists beyond 6 months. However, vascular function at the segment of the stent was preserved, thereby confirming endothelial recovery. The recovery of the functionality of the endothelium, as observed at 1 month with complete endothelial coverage at 6 months, may maintain the vasoprotective effect^{48,49}. In addition, the long-term outcomes of the use of our proposed stent are unknown, and further studies with a long follow-up period are warranted.

Conclusions

We developed a biodegradable “cable-tie” type eluting rapamycin nanofiber stent. The design included a self-locking mechanism and the ability to avoid stent recoil resulted from polymer properties and external pressure of blood vessels. The fabricated cable-tie stents exhibited excellent mechanical properties on evaluation of compression test and collapse pressure, and less than 8% weight loss following being immersed in PBS for 16 weeks. Furthermore, the biodegradable stents delivered high rapamycin concentrations for over 4 weeks and achieved substantial reductions in intimal hyperplasia associated with elevated heme oxygenase-1 and calponin level on the denuded rabbit arteries during 6 months of follow-up. The cable-tie type stents developed in this study might have high potential impacts for the local drug delivery to treat various vascular diseases.

References

- Wald, D. S. *et al.* Randomized trial of preventive angioplasty in myocardial infarction. *The New England journal of medicine* **369**, 1115–1123 (2013).
- O’Gara, P. T. *et al.* 2013 ACCF/AHA guideline for the management of ST-elevation myocardial infarction: executive summary: a report of the American College of Cardiology Foundation/American Heart Association Task Force on Practice Guidelines. *Circulation* **127**, 529–555 (2013).
- Task Force on Myocardial Revascularization of the European Society of Cardiology, *et al.* Guidelines on myocardial revascularization. *European heart journal* **31**, 2501–2555, (2010).
- Pfisterer, M. *et al.* Late clinical events after clopidogrel discontinuation may limit the benefit of drug-eluting stents: an observational study of drug-eluting versus bare-metal stents. *Journal of the American College of Cardiology* **48**, 2584–2591 (2006).
- McFadden, E. P. *et al.* Late thrombosis in drug-eluting coronary stents after discontinuation of antiplatelet therapy. *Lancet* **364**, 1519–1521 (2004).
- Virmani, R. *et al.* Localized hypersensitivity and late coronary thrombosis secondary to a sirolimus-eluting stent: should we be cautious? *Circulation* **109**, 701–705 (2004).
- Joner, M. *et al.* Pathology of drug-eluting stents in humans: delayed healing and late thrombotic risk. *Journal of the American College of Cardiology* **48**, 193–202 (2006).
- Nakazawa, G. *et al.* Delayed arterial healing and increased late stent thrombosis at culprit sites after drug-eluting stent placement for acute myocardial infarction patients: an autopsy study. *Circulation* **118**, 1138–1145 (2008).
- Gammon, R. S. *et al.* Mechanical features of the duke biodegradable intravascular stent. *Journal of the American College of Cardiology* **17**, A235–A235 (1991).
- Tamai, H. *et al.* Initial and 6-month results of biodegradable poly-L-lactic acid coronary stents in humans. *Circulation* **102**, 399–404 (2000).
- Venkatraman, S. S., Tan, L. P., Joso, J. F., Boey, Y. C. & Wang, X. Biodegradable stents with elastic memory. *Biomaterials* **27**, 1573–1578 (2006).
- Chen, M. C. *et al.* Rapidly self-expandable polymeric stents with a shape-memory property. *Biomacromolecules* **8**, 2774–2780 (2007).
- Liu, S. J., Chiang, F. J., Hsiao, C. Y., Kau, Y. C. & Liu, K. S. Fabrication of balloon-expandable self-lock drug-eluting polycaprolactone stents using micro-injection molding and spray coating techniques. *Annals of biomedical engineering* **38**, 3185–3194 (2010).
- Meredith, I. T. *et al.* Primary endpoint results of the EVOLVE trial: a randomized evaluation of a novel bioabsorbable polymer-coated, everolimus-eluting coronary stent. *J Am Coll Cardiol* **59**, 1362–1370 (2012).
- Serruys, P. W. *et al.* A bioabsorbable everolimus-eluting coronary stent system (ABSORB): 2-year outcomes and results from multiple imaging methods. *Lancet* **373**, 897–910 (2009).
- Tanimoto, S. *et al.* Late stent recoil of the bioabsorbable everolimus-eluting coronary stent and its relationship with plaque morphology. *J Am Coll Cardiol* **52**, 1616–1620 (2008).
- Mattessini, A. *et al.* ABSORB biodegradable stents versus second-generation metal stents: a comparison study of 100 complex lesions treated under OCT guidance. *JACC. Cardiovascular interventions* **7**, 741–750 (2014).
- Fernandez-Rodriguez, D., Brugaletta, S., Otsuki, S. & Sabate, M. Acute Absorb bioresorbable vascular scaffold thrombosis in ST-segment elevation myocardial infarction: to stent or not to stent? *EuroIntervention: journal of EuroPCR in collaboration with the Working Group on Interventional Cardiology of the European Society of Cardiology* **10**, 600 (2014). discussion 600.
- Kohn, C. G., Kluger, J., Azeem, M. & Coleman, C. I. Short-term consequences of angiographically-confirmed coronary stent thrombosis. *PLoS one* **8**, e77330 (2013).
- Lee, C. H. *et al.* Promoting endothelial recovery and reducing neointimal hyperplasia using sequential-like release of acetylsalicylic acid and paclitaxel-loaded biodegradable stents. *International journal of nanomedicine* **9**, 4117–4133 (2014).
- Lee, C. H. *et al.* Local sustained delivery of acetylsalicylic acid via hybrid stent with biodegradable nanofibers reduces adhesion of blood cells and promotes reendothelialization of the denuded artery. *International journal of nanomedicine* **9**, 311–326 (2014).
- Lee, C. H. *et al.* Acceleration of re-endothelialization and inhibition of neointimal formation using hybrid biodegradable nanofibrous rosvastatin-loaded stents. *Biomaterials* **35**, 4417–4427 (2014).
- Kornowski, R. *et al.* In-stent restenosis: contributions of inflammatory responses and arterial injury to neointimal hyperplasia. *J Am Coll Cardiol* **31**, 224–230 (1998).
- Schwartz, R. S. *et al.* Restenosis and the proportional neointimal response to coronary artery injury: results in a porcine model. *J Am Coll Cardiol* **19**, 267–274 (1992).
- Nakazawa, G. *et al.* Anti-CD34 antibodies immobilized on the surface of sirolimus-eluting stents enhance stent endothelialization. *JACC Cardiovasc Interv* **3**, 68–75 (2010).

26. Drolet, M. C., Plante, E., Battistini, B., Couet, J. & Arseneault, M. Early endothelial dysfunction in cholesterol-fed rabbits: a non-invasive *in vivo* ultrasound study. *Cardiovasc Ultrasound* **2**, 10 (2004).
27. Nakamura, S. *et al.* Intracoronary ultrasound observations during stent implantation. *Circulation* **89**, 2026–2034 (1994).
28. Mak, K. H., Belli, G., Ellis, S. G. & Moliterno, D. J. Subacute stent thrombosis: evolving issues and current concepts. *Journal of the American College of Cardiology* **27**, 494–503 (1996).
29. Serruys, P. W. *et al.* A comparison of balloon-expandable-stent implantation with balloon angioplasty in patients with coronary artery disease. Benestent Study Group. *The New England journal of medicine* **331**, 489–495 (1994).
30. Kuntz, R. E., Gibson, C. M., Nobuyoshi, M. & Baim, D. S. Generalized model of restenosis after conventional balloon angioplasty, stenting and directional atherectomy. *Journal of the American College of Cardiology* **21**, 15–25 (1993).
31. Al Suwaidi, J., Higano, S. T., Holmes, D. R. Jr., Rihal, C. S. & Lerman, A. Measuring maximal percent area stenosis poststent placement with intracoronary Doppler and the continuity equation and correlation with intracoronary ultrasound and angiography. *The American journal of cardiology* **84**, 650–654 (1999).
32. Rieu, R. *et al.* Radial force of coronary stents: a comparative analysis. *Catheterization and cardiovascular interventions: official journal of the Society for Cardiac Angiography & Interventions* **46**, 380–391 (1999).
33. Su, S. H. *et al.* Expandable bioresorbable endovascular stent. I. Fabrication and properties. *Annals of biomedical engineering* **31**, 667–677 (2003).
34. deployment, a. o. m. s. *et al.* Ciprofloxacin-impregnated poly-L-lactic acid drug carrier. New aspects of a resorbable drug delivery system in local antimicrobial treatment of bone infections. *Archives of orthopaedic and trauma surgery* **112**, 33–35, (1992).
35. Wang, Z., Wang, Y., Ito, Y., Zhang, P. & Chen, X. A comparative study on the *in vivo* degradation of poly(L-lactide) based composite implants for bone fracture fixation. *Scientific reports* **6**, 20770 (2016).
36. Axel, D. I. *et al.* Paclitaxel inhibits arterial smooth muscle cell proliferation and migration *in vitro* and *in vivo* using local drug delivery. *Circulation* **96**, 636–645 (1997).
37. Pires, N. M. *et al.* Local perivascular delivery of anti-restenotic agents from a drug-eluting poly(epsilon-caprolactone) stent cuff. *Biomaterials* **26**, 5386–5394 (2005).
38. Venkatraman, S., Poh, T. L., Vinalia, T., Mak, K. H. & Boey, F. Collapse pressures of biodegradable stents. *Biomaterials* **24**, 2105–2111 (2003).
39. Alexis, F., Venkatraman, S. S., Rath, S. K. & Boey, F. *In vitro* study of release mechanisms of paclitaxel and rapamycin from drug-incorporated biodegradable stent matrices. *Journal of controlled release: official journal of the Controlled Release Society* **98**, 67–74 (2004).
40. Hancock, W. W., Buelow, R., Sayegh, M. H. & Turka, L. A. Antibody-induced transplant arteriosclerosis is prevented by graft expression of anti-oxidant and anti-apoptotic genes. *Nature medicine* **4**, 1392–1396 (1998).
41. Duckers, H. J. *et al.* Heme oxygenase-1 protects against vascular constriction and proliferation. *Nature medicine* **7**, 693–698 (2001).
42. Visner, G. A. *et al.* Rapamycin induces heme oxygenase-1 in human pulmonary vascular cells: implications in the antiproliferative response to rapamycin. *Circulation* **107**, 911–916 (2003).
43. Birukov, K. G., Stepanova, O. V., Nanaev, A. K. & Shirinsky, V. P. Expression of calponin in rabbit and human aortic smooth muscle cells. *Cell and tissue research* **266**, 579–584 (1991).
44. Horowitz, A. *et al.* Effects of calponin on force generation by single smooth muscle cells. *The American journal of physiology* **270**, H1858–1863 (1996).
45. Yamamura, H., Ikeda, W., Shibata, N., Awata, N. & Takahashi, K. In *The Ischemic Heart* (eds Seibu Mochizuki, Nobuakira Takeda, Makoto Nagano & Naranjan S. Dhalla) 87–95 (Springer US, 1998).
46. Martin, K. A. *et al.* Rapamycin promotes vascular smooth muscle cell differentiation through insulin receptor substrate-1/ phosphatidylinositol 3-kinase/Akt2 feedback signaling. *The Journal of biological chemistry* **282**, 36112–36120 (2007).
47. Hegner, B., Weber, M., Dragun, D. & Schulze-Lohoff, E. Differential regulation of smooth muscle markers in human bone marrow-derived mesenchymal stem cells. *Journal of hypertension* **23**, 1191–1202 (2005).
48. Rosenson, R. S. & Tangney, C. C. Antiatherothrombotic properties of statins: implications for cardiovascular event reduction. *JAMA* **279**, 1643–1650 (1998).
49. Celik, T., Iyisoy, A., Kursaklioglu, H. & Celik, M. The forgotten player of in-stent restenosis: endothelial dysfunction. *Int J Cardiol* **126**, 443–444 (2008).

Acknowledgements

This study was supported by the Ministry of Science and Technology (Taiwan) (Contract No NSC-105-2314-B-182A-098-MY2) and Chang Gung Memorial Hospital (Contract No CMRPG3F0891 and CMRPD3D0153) for financially supporting this research.

Author Contributions

C.H.L., S.H.C., and M.J.H. designed the study, analysed the data and drafted the manuscript. C.C.C., C.L.C., P.C.C., and C.L.F. interpreted the data and drafted and critically revised the manuscript for important intellectual content. W.J.C., C.J.W., M.Y.H., and K.C.H. contributed to the study design and reviewed, edited and critically revised the manuscript. S.J.L. had full access to all data in the study and takes responsibility for the integrity of the data and the accuracy of the data analysis. All authors gave final approval of the final vision to be published. The manuscript represents valid work and neither this manuscript nor one with substantially similar content under their authorship has been published or is being considered for publication elsewhere. Data are available on request from the corresponding author.

Additional Information

Supplementary information accompanies this paper at doi:10.1038/s41598-017-00131-w

Competing Interests: The authors declare that they have no competing interests.

Publisher's note: Springer Nature remains neutral with regard to jurisdictional claims in published maps and institutional affiliations.



This work is licensed under a Creative Commons Attribution 4.0 International License. The images or other third party material in this article are included in the article's Creative Commons license, unless indicated otherwise in the credit line; if the material is not included under the Creative Commons license, users will need to obtain permission from the license holder to reproduce the material. To view a copy of this license, visit <http://creativecommons.org/licenses/by/4.0/>

© The Author(s) 2017